Scale Separation of Shear-Induced Criticality in Glasses

Norihiro Oyama,[1,*] Takeshi Kawasaki,[2] Kang Kim,[3] and Hideyuki Mizuno[4]
[1]Toyota Central R&D Labs., Inc., Nagakute 480-1192, Japan
[2]Department of Physics, Nagoya University, Nagoya 464-8602, Japan
[3]Division of Chemical Engineering, Department of Materials Engineering Science, Graduate School of Engineering Science, Osaka University, Toyonaka, Osaka 560-8531, Japan
[4]Graduate School of Arts and Sciences, The University of Tokyo, Tokyo 153-8902, Japan

(Received 17 October 2023; revised 30 December 2023; accepted 21 February 2024; published 3 April 2024)

In a sheared steady state, glasses reach a nonequilibrium criticality called *yielding criticality*. We report that the qualitative nature of this nonequilibrium critical phenomenon depends on the details of the system and that responses and fluctuations are governed by different critical correlation lengths in specific situations. This scale separation of critical lengths arises when the screening of elastic propagation of mechanical signals is not negligible. We also discuss the determinant of the impact of screening effects from the viewpoint of the microscopic dissipation mechanism.

DOI: 10.1103/PhysRevLett.132.148201

Introduction.—In athermal (zero-temperature) sheared glasses, fluidization proceeds through many local plastic events [1–18]. In a steady state, in particular, the elementary processes of these plastic events, so-called shear transformations (STs), tend to form avalanches [2,3,17]. Such avalanches can sometimes span the whole system and result in one class of nonequilibrium criticality [19] called *yielding criticality* [15,17,20]. The criticality is typically reflected by stress response: the average stress $\langle\sigma\rangle$ obeys a critical phenomenonlike functional form called the Herschel-Bulkley (HB) law $\langle\sigma\rangle - \sigma_Y \sim \dot{\gamma}^n$ [21] and exhibits a finite size effect [5,6,9,17]. Here, σ_Y is the yield stress, $\dot{\gamma}$ is the applied strain rate, and n is the HB exponent. This yielding criticality is also characterized by scaling *Ansätze* [17,20] $\xi \sim |\langle\sigma\rangle - \sigma_Y|^{-\nu}$ and $\dot{\gamma} \sim |\langle\sigma\rangle - \sigma_Y|^{\beta}$, where ξ is the critical correlation length of avalanches and ν and β are critical exponents. From the statistical tilt symmetry of the governing equation, we can show that the exponent ν has a hyperscaling relation $\nu = 1/(d - d_f)$ with the fractal dimension d_f of the geometric structure of avalanches [20]. The fractal dimension d_f and the yield stress σ_Y [22] can be determined by simulations under quasistatic shear [16,17,20]. From the above scaling relation, we can further determine ν.

Although there was no way to measure the remaining important parameter β systematically in particulate systems, we recently found that we can obtain β from the average number of STs occurring simultaneously $\langle N_{ST}\rangle$. We can describe $\langle N_{ST}\rangle$ as

$$\langle N_{ST}\rangle \sim N_{ava} \times N_{ST/ava} \sim N \times \dot{\gamma}^{1/\beta}, \tag{1}$$

where N_{ava} and $N_{ST/ava}$ represent the number of avalanches in the system and the number of STs in each avalanche, respectively. By definition, they can be expressed as $N_{ava} \sim (L/\xi)^d$ and $N_{ST/ava} \sim \xi^{d_f}$ [17] [see Supplemental Material (SM) [23] for a detailed explanation]. Using Eq. (1), we can determine β from the $\dot{\gamma}$ dependence of the average number density of STs $\langle n_{ST}\rangle \equiv \langle N_{ST}\rangle/N$. Furthermore, we found that instantaneous normal modes with imaginary frequencies (we call them Im-INMs) correspond to activated STs that are causing plastic deformations [17], and thus N_{ST} can be estimated from the number of Im-INMs. Instantaneous normal modes are obtained as the eigenmodes of the Hessian matrix of the total potential energy of an instantaneous configuration [25–29], which is available in particulate systems. Therefore, the important parameters to characterize yielding criticality, σ_Y, ν, and β, can all be determined systematically. In Ref. [17], we demonstrated that the estimated parameters describe well the criticality of the numerically observed stress and established the validity of the concept of yielding criticality.

Moreover, in sheared glasses, the dynamics of constituent particles become diffusive even under athermal conditions [4,5,8,9,12]. If we quantify diffusive motions by the strain-based diffusion constant $\hat{D}$, they also exhibit criticality as $\hat{D} \sim \dot{\gamma}^{-n_{\hat{D}}}$. Here, we introduced a critical exponent $n_{\hat{D}}$ and defined the diffusion constant as $\hat{D} \equiv \hat{\Delta}^2(\gamma_t \to \infty)$ using the strain-based mean-squared displacements in the y direction, $\hat{\Delta}^2(\gamma_t) \equiv \langle (1/N)\sum_i [y_i(0) - y_i(t)]^2\rangle/\gamma_t$. We assume that the system is two dimensional (2D) [4,5,8,9] and that the shear is applied in the x direction. $\gamma_t \equiv \dot{\gamma}t$ is the strain applied during a time interval t. The precise measurements of the exponent $n_{\hat{D}}$, including the confirmation by finite size scaling (FSS), were performed in Refs. [5,9]. In particular, in Ref. [5], based on a general phenomenological discussion, a theoretical prediction for

the exponent was given as $n_{\hat{D}} = 1/2$, which is in line with the numerical result. This prediction was considered not to depend on the system details according to the general nature of the theoretical treatment. However, Ref. [9] reported a largely different value of $n_{\hat{D}} = 1/3$ under a different numerical setup. We lack an understanding of the cause of this unexpected diversity of $n_{\hat{D}}$.

In this Letter, we study the cause of the diversity in $n_{\hat{D}}$ by means of molecular dynamics simulations of 2D sheared glasses and the scaling argument based on the recently established yielding criticality. Our main finding is that there are not only quantitative differences in the values of exponents but also qualitative differences in the property of the criticality itself. We first found that $n_{\hat{D}}$ is inversely proportional to β. Since the diversity of β is already known [30,31], this inverse proportionality explains the diversity in $n_{\hat{D}}$ reported thus far [5,9]. By comparing the results for two systems with qualitatively different microscopic dissipation mechanisms, however, we found that $n_{\hat{D}}$ can also be largely different even when β is nearly the same. This unexpected diversity in $n_{\hat{D}}$ arises because the diverging correlation length governing the criticality of diffusion differs from that governing stress in one system while, in the other system, such a scale separation is absent. We further clarified the physical meaning of the second critical correlation length governing the diffusion and the reason why such scale separation could be observed only under certain conditions.

Numerical setups.—We conduct molecular dynamics simulations of 2D ($d = 2$) glasses under external shear. The interparticle interaction follows from the Lennard-Jones potential with smoothing terms [16,17] which ensure that the potential and force smoothly tend to zero at the cutoff distance $r_{ij}^c = 1.3d_{ij}$, where d_{ij} determines the interaction range between particles i and j. To avoid crystallization, we consider a 50:50 mixture of two types of particles with different sizes but with the same mass $m = 1.0$. The interaction ranges for different pairs of particle types are $d_{\mathrm{SS}} = 5/6$, $d_{\mathrm{SL}} = 1.0$, and $d_{\mathrm{LL}} = 7/6$, where subscripts S and L distinguish particle types. The energy scale $\epsilon_{ij} = \epsilon = 1.0$ is constant for all particle pairs. The physical variables reported in this Letter are all nondimensionalized by d_{SL}, m, and ϵ. The number density ρ is set to be $\rho = N/L^2 \sim 1.09$, where N is the number of particles and L is the corresponding linear dimension of the system.

We applied the shear at different rates in the range of $2 \times 10^{-5} \leq \dot{\gamma} \leq 2 \times 10^{-2}$. At every simulation step, we first impose affine simple shear of strain $\Delta\gamma$ in the x direction and then calculate the nonaffine dynamics for a time interval of Δt by integrating the equations of motion under the Lees-Edwards boundary conditions [32]. The shear rate is expressed as $\dot{\gamma} = \Delta\gamma/\Delta t$. To make the strain resolution constant, we fix $\Delta\gamma$ to be 1.0×10^{-7} and control $\dot{\gamma}$ by changing the time step Δt. Since the speed of sound in our system is approximately unity, our simulations with these setups resolve the elastic wave propagation process with a sufficiently fine resolution [33].

We considered two types of systems, systems A and B, that have different microscopic dissipation mechanisms. (i) System A: "Contact" damping. In system A, dissipative interparticle forces are introduced as $\boldsymbol{f}_i^{\mathrm{visc}} = (m/\tau)\sum_j \phi(r_{ij})(\delta\boldsymbol{v}_j - \delta\boldsymbol{v}_i)$ [5]. Here, $\phi(r_{ij}) \propto 1\text{–}2(r_{ij}/r_{ij}^{\mathrm{C}})^4 + (r_{ij}/r_{ij}^{\mathrm{C}})^8$ is a smoothing function, $\delta\boldsymbol{v}_i$ is the nonaffine velocity, and $\tau = 0.2$ is the dissipation timescale. This type of dissipation selectively damps high-wave-number local relative motions [34]. (ii) System B: Stokes drag. In system B, the dissipation is modeled through the Stokes drag force as $\boldsymbol{f}_i^{\mathrm{drag}} = -\Gamma\delta\boldsymbol{v}_i$ [35,36], where the damping coefficient Γ is set to unity.

Averages are denoted by angular brackets $\langle\cdot\rangle$ and they are calculated over steady-state data ($1 \leq \gamma \leq 20$) and 8 independent samples. Initial configurations are all generated by the minimization of the potential energy of totally random structures. We ignore the thermal fluctuations (athermal situation).

Scaling argument for diffusion constant.—We plot the strain-based diffusion constant $\hat{D}$ for different system sizes N as functions of the shear rate $\dot{\gamma}$ in Figs. 1(a) and 1(b). In the low $\dot{\gamma}$ regime below a system-size dependent threshold $\dot{\gamma}_{C_{\hat{D}}}$, $\hat{D}$ plateaus at $\hat{D}_0$. The plateau value $\hat{D}_0$ also linearly depends on the system linear dimension L as $\hat{D}_0 \sim L$ [37]. In the high-rate limit, on the other hand, $\hat{D}$ seems to obey characteristic power laws. All these behaviors are common to both systems A and B and consistent with reports in Refs. [5,9].

To describe the critical behavior of $\hat{D}$ in the framework of the yielding criticality, we introduce another scaling *Ansatz* with a new exponent α as $\hat{D} \sim \Delta\sigma^{-\alpha} \sim \dot{\gamma}^{-\alpha/\beta}$. Introducing a scaling function $f_{\hat{D}}(x)$, we obtain $\hat{D} \times \dot{\gamma}_{C_{\hat{D}}}^{\alpha/\beta} = (\dot{\gamma}/\dot{\gamma}_{C_{\hat{D}}})^{-\alpha/\beta} f_{\hat{D}}(\dot{\gamma}/\dot{\gamma}_{C_{\hat{D}}})$. On the other hand, we can also describe $\hat{D}$ using the critical correlation length ξ as $\hat{D} \sim \xi^{\alpha/\nu}$. Because $\hat{D}$ becomes $\hat{D}_0$ at $\dot{\gamma} = \dot{\gamma}_{C_{\hat{D}}}$, we obtain a relation $L^{\alpha/\nu} \sim \hat{D}_0 \sim L$ and $\dot{\gamma}_{C_{\hat{D}}} \sim L^{-\beta/\nu}$ (see SM for details [23]). From all these relations, we obtain $\alpha = \nu$ and

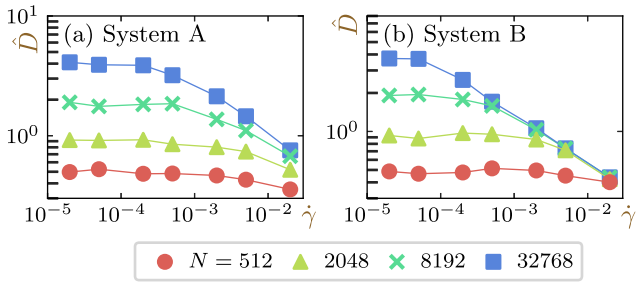

FIG. 1. Strain-based diffusion constant $\hat{D}$ as a function of $\dot{\gamma}$. Results for (a) system A and (b) system B.

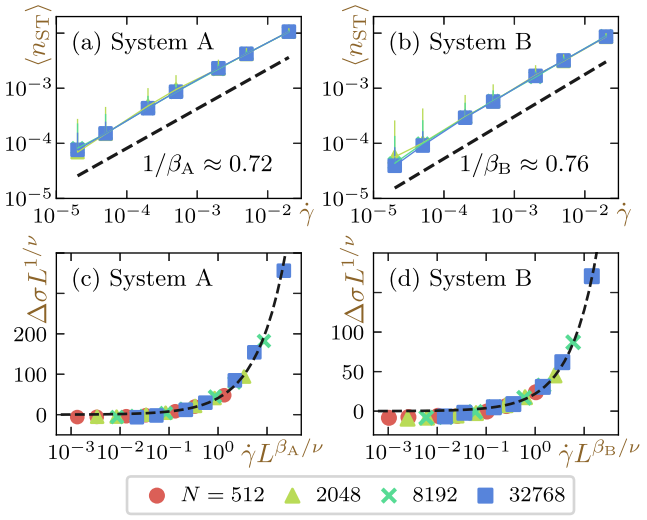

FIG. 2. (a),(b) Average number density of STs $\langle n_{ST} \rangle$ as a function of the shear rate $\dot{\gamma}$. The dashed lines are the fitting results using all data points and have slopes of $1/\beta_A \approx 0.72$ and $1/\beta_B \approx 0.76$. (c),(d) $\Delta\sigma \equiv \langle \sigma \rangle - \sigma_Y$ as a function of shear rate with finite size scaling. The dashed lines show the HB law: $\Delta\sigma \sim \dot{\gamma}^{1/\beta_{A/B}}$. Left: results for system A. Right: results for system B.

$$\hat{D}/L = (L \times \dot{\gamma}^{\nu/\beta})^{-1} f_{\hat{D}}(\dot{\gamma}/\dot{\gamma}_{C_{\hat{D}}}). \tag{2}$$

Therefore, with correct values of ν and β, we expect the FSS according to this equation to collapse curves of $\hat{D}$ for different system sizes. Additionally, by comparing the exponents, we obtain a relation $n_{\hat{D}} = \nu/\beta$. These results mean that the criticality of $\hat{D}$ can be described only by β and ν, the exponents introduced to describe the criticality of the stress response.

Measurement of exponents and yield stress.—As explained above, we can extract the precise values of β from $\langle n_{ST} \rangle$, the average number density of STs. In Figs. 2(a) and 2(b), we plot $\langle n_{ST} \rangle$ estimated by the number of Im-INMs [17] as a function of $\dot{\gamma}$ for systems A and B. As expected from Eq. (1), $\langle n_{ST} \rangle$ does not show any system-size dependence, and the results for all system sizes obey a master power-law curve for both systems. From the slopes, we can determine the values of β as $\beta_A \approx 1.39$ and $\beta_B \approx 1.32$, where subscripts A and B distinguish the system of interest (we summarize all values of critical exponents in Table I). We note that although β_A and β_B happened to be close, the value of the HB exponent $n = 1/\beta$ generally depends on the details of the system, with values as varied as $0.2 \leq n \leq 0.8$ being reported [30,31].

Moreover, we can determine σ_Y and d_f from the data in the quasistatic limit obeying the procedure introduced in Ref. [20]. We note that, while the value of d_f is shared by the two systems and is consistent with that obtained from the athermal quasistatic simulation [16] [$d_f \approx 1.03$ and, thus, $\nu = 1/(d - d_f) \approx 1.04$], interestingly, we found that the values of the yield stress were slightly different between the two systems: $\sigma_Y^A \approx 3.66$ and $\sigma_Y^B \approx 3.75$ [17] (see SM for details [23]). We demonstrate the success of FSS of $\Delta\sigma \equiv \langle \sigma \rangle - \sigma_Y$ with these parameters in Figs. 2(c) and 2(d) for systems A and B, respectively. These results guarantee the correctness of exponents $\beta_{A/B}$ and ν.

We now try an FSS of $\hat{D}$ using the obtained exponents and Eq. (2): the results are shown in Fig. 3. As shown in Fig. 3(a), for system A, the results for different N collapse. This indicates that $\hat{D}$ is governed by ξ, and thus $n_{\hat{D},A}$ is estimated as $n_{\hat{D},A} = \nu/\beta_A \approx 0.72$. We note that, in systems of both Refs. [5,9], the criticalities of $\hat{D}$ were described by ξ as well, as explained in detail in SM [23]. This means that the variation in $n_{\hat{D}}$ among these systems simply derives from that in $n = 1/\beta$ ($n = 1/2$ [5] and $1/3$ [9]).

On the other hand, as shown in Fig. 3(b), the FSS is not successful for system B: the data in the high-shear-rate scaling regime vary significantly among different N. The failure of this attempt is due to the inadequacy of the implicit assumption in Eq. (2) that the criticality of $\hat{D}$ and $\langle \sigma \rangle$ are governed by the same correlation length ξ. Below, we explain that there exists another critical correlation length and that the second length governs the criticality of $\hat{D}$ in system B.

Existence of another length scale.—In the phenomenological discussion in Refs. [5,12], $\hat{D}$ was described by a superposition of Eshelby fields [38] induced by all STs in the system (see SM for a brief summary of the theoretical background [23]). Importantly, to reproduce the critical finite size effect, the correlation between STs over the length scale ξ was crucial. In this phenomenological consideration, the effect of each Eshelby field was assumed to propagate throughout the whole system via an elastic field.

TABLE I. Summary of exponents and scaling *Ansätze*.

Exponent	Corresponding variable	Definition	Measurement	System A	System B
β	Shear rate	$\dot{\gamma} \sim \Delta\sigma^{\beta}$	INMs analysis [17]	1.39	1.32
d_f	Avalanche size	$S \sim \xi^{d_f}$	Quasistatic simulations [16]	1.03	
ν	Avalanche correlation length	$\xi \sim \Delta\sigma^{-\nu}$	$\nu = 1/(d - d_f)$ [20]	1.04	
$\tilde{\nu}$	ST correlation length	$\zeta \sim \Delta\sigma^{-\tilde{\nu}}$	$\tilde{\nu} = 1/d$	0.50	
$n_{\hat{D}}$	Diffusion constant	$\hat{D} \sim \dot{\gamma}^{-n_{\hat{D}}}$	$n_{\hat{D},A} = \nu/\beta_A$, $n_{\hat{D},B} = \tilde{\nu}/\beta_B$	0.74	0.38

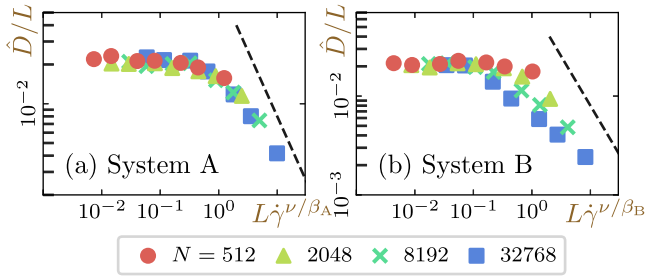

FIG. 3. Finite size scaling of strain-based diffusion constant $\hat{D}$ using exponent $\nu \approx 1.04$ associated with the avalanche correlation length ξ. Dashed lines represent the slope of -1 expected from the scaling argument. Results for (a) system A and (b) system B.

When there are multiple excited STs in the system, however, this assumption may not always hold. If we consider the displacement of a particle induced by Eshelby fields, the local plastic motion of nearby STs can screen the elastic propagation of Eshelby fields emitted by distant STs [39]. Therefore, when such screening effects cannot be ignored, the length scale over which elastic waves can travel without interference from other STs plays a major role in determining the diffusivity. We name such a length scale ζ and assume another scaling *Ansatz* for it as $\zeta \sim \Delta\sigma^{-\tilde{\nu}}$, introducing another exponent $\tilde{\nu}$. If the criticality of $\hat{D}$ is governed by ζ, we obtain $\alpha = \tilde{\nu}$ and $\hat{D}/L = (L \times \dot{\gamma}^{\tilde{\nu}/\beta})^{-1} g_{\hat{D}}(\dot{\gamma}/\dot{\gamma}_{C_{\hat{D}}})$ from the same derivation of Eq. (2) (see also SM) [23].

To consider the finite size scaling of $\hat{D}$ by ζ, we need to estimate $\tilde{\nu}$. For this, $\langle N_{\mathrm{ST}} \rangle$ can be utilized again. The length scale ζ corresponds to the linear dimension of the average volume occupied by a single ST [see a schematic picture in Fig. 4(a); we call ζ the ST correlation length hereafter]. Thus, the exponent $\tilde{\nu}$ can be determined by considering a situation where $\langle N_{\mathrm{ST}} \rangle \sim \zeta^d \dot{\gamma}^{1/\beta} \sim 1$ [from Eq. (1) with $L = \zeta$]. We obtain $\tilde{\nu} = 1/d$ from this relation (see SM for details [23]). Since the two exponents, $\nu \approx 1.0$ and $\tilde{\nu} = 1/d = 1/2$, are largely different, the corresponding lengths ξ and ζ are different in nature in view of the critical phenomena. As a reference, we show the sketch for the avalanche correlation length ξ in Fig. 4(b). As shown here, ξ corresponds to, by definition, the overall spanning length of avalanches formed by STs (see SM for a precise definition).

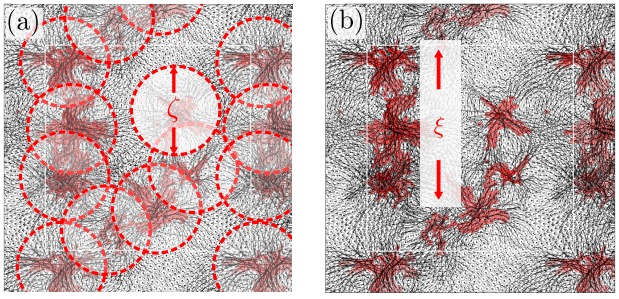

FIG. 4. Schematic picture of (a) ST correlation length ζ and (b) avalanche correlation length ξ. Mobile particles (see SM for precise definition [23]) of all Im-INMs that correspond to active STs are highlighted in red. The results from a system with $N = 2048$ under shear of the rate $\dot{\gamma} = 2 \times 10^{-3}$ are shown. The copied images due to the periodic boundary conditions are also visualized around the original computational domain with lighter colors. Black arrows depict the eigenvectors.

In Fig. 5(a), we plot the results of the FSS of $\hat{D}$ using the critical exponent $\tilde{\nu}$ for system A: the scaling is obviously not successful. This failure allows us to reconfirm that the criticality of $\hat{D}$ is governed solely by ξ, not by ζ. In Fig. 5(b), we tried the same FSS for system B. In this case, we see a perfect collapse of results for different N and can conclude that $\hat{D}$ is governed by ζ. In other words, in this system, separation of the critical correlation lengths is observed between criticalities of $\langle \sigma \rangle$ (a measure of response) and $\hat{D}$ (a measure of fluctuations): Since fluctuations are locally determined, they are affected by screening effects, whereas the response is globally determined by the total spanning length of avalanches and is therefore independent of screening effects. Because this scale separation is present only in system B, even though $\beta_A \approx 1.39$ and $\beta_B \approx 1.32$ are close, $n_{\hat{D},A} \approx 0.72$ and $n_{\hat{D},B} \approx 0.38$ are largely different.

An important question remains: Why is the screening effect negligible in system A? This is likely because high-wave-number local relative motions are overdamped in this system [34]. Because of this feature, local motions resulting from the excitation of STs are suppressed and the screening effect of elastic wave propagation becomes very weak. We note that, as we explain in detail in SM [23], reinterpretation of reported values of exponents in Refs. [5,9] indicates that the scale separation is also negligible in the systems in these studies. The high-wave-number motions are overdamped in those systems in Refs. [5,9] as well, which is consistent with the discussion in this paragraph.

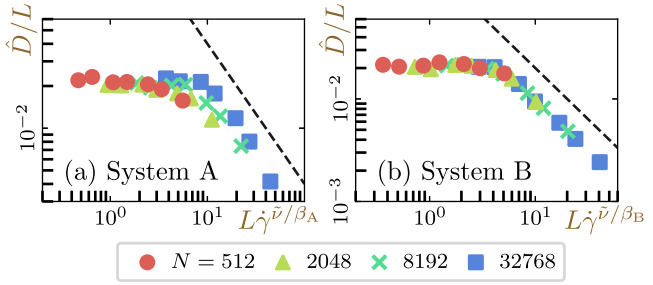

FIG. 5. Finite size scaling of the strain-based diffusion constant $\hat{D}$ using the exponent $\tilde{\nu} = 1/d$ associated with the ST correlation length ζ. Dashed lines represent the slope of -1 expected from the scaling argument. (a) Results for system A. (b) Results for system B.

Summary and overview.—In this Letter, by means of molecular dynamics simulations of sheared 2D glasses, we studied the origin of the diversity of exponent $n_{\hat{D}}$ characterizing the criticality of the diffusion coefficient, which had remained previously unclear. We found that the diversity in $n_{\hat{D}}$ was caused not only by quantitative but also by qualitative differences: whether the scale separation of the critical correlation lengths of response and fluctuation is present or not. We also revealed that the screening effect of elastic waves, which arises when microscopic dissipation does not completely damp high-wave-number local dynamics, is responsible for the emergence of such scale separation.

We mention that the presence of multiple critical correlation lengths is also reported for other critical phenomena such as jamming [40] and quantum phase transitions [41], although the origins of the scale separation are distinct among the examples. In the future, other critical phenomena with scale separation may be discovered, and it may become possible to classify the separation mechanisms into several classes.

The authors thank Masanari Shimada for fruitful discussions. This work was financially supported by the JST FOREST Program (Grant No. JPMJFR212T) and JSPS KAKENHI Grants No. JP20H01868, No. JP22H04472, No. JP22K03543, No. JP23H04495, No. JP23H04503, and No. JP22K03550.

*Norihiro.Oyama.vb@mosk.tytlabs.co.jp

[1] C. Maloney and A. Lemaître, Universal breakdown of elasticity at the onset of material failure, Phys. Rev. Lett. **93**, 195501 (2004).
[2] C. Maloney and A. Lemaître, Subextensive scaling in the athermal, quasistatic limit of amorphous matter in plastic shear flow, Phys. Rev. Lett. **93**, 016001 (2004).
[3] C. E. Maloney and A. Lemaître, Amorphous systems in athermal, quasistatic shear, Phys. Rev. E **74**, 016118 (2006).
[4] A. Lemaître and C. Caroli, Plastic response of a two-dimensional amorphous solid to quasistatic shear: Transverse particle diffusion and phenomenology of dissipative events, Phys. Rev. E **76**, 036104 (2007).
[5] A. Lemaître and C. Caroli, Rate-dependent avalanche size in athermally sheared amorphous solids, Phys. Rev. Lett. **103**, 065501 (2009).
[6] T. Hatano, Rheology and dynamical heterogeneity in frictionless beads at jamming density, J. Phys. Conf. Ser. **319**, 012011 (2011).
[7] S. Karmakar, E. Lerner, and I. Procaccia, Statistical physics of the yielding transition in amorphous solids, Phys. Rev. E **82**, 055103(R) (2010).
[8] K. Martens, L. Bocquet, and J.-L. Barrat, Connecting diffusion and dynamical heterogeneities in actively deformed amorphous systems, Phys. Rev. Lett. **106**, 156001 (2011).
[9] A. P. Roy, K. Karimi, and C. E. Maloney, Rheology, diffusion, and velocity correlations in the bubble model, arXiv:1508.00810.
[10] M. Ozawa, L. Berthier, G. Biroli, A. Rosso, and G. Tarjus, Random critical point separates brittle and ductile yielding transitions in amorphous materials, Proc. Natl. Acad. Sci. U.S.A. **115**, 6656 (2018).
[11] D. Zhang, K. A. Dahmen, and M. Ostoja-Starzewski, Scaling of slip avalanches in sheared amorphous materials based on large-scale atomistic simulations, Phys. Rev. E **95**, 032902 (2017).
[12] K. Karimi, Self-diffusion in plastic flow of amorphous solids, Phys. Rev. E **100**, 063003 (2019).
[13] N. Oyama, H. Mizuno, and K. Saitoh, Avalanche interpretation of the power-law energy spectrum in three-dimensional dense granular flow, Phys. Rev. Lett. **122**, 188004 (2019).
[14] K. Saitoh, N. Oyama, F. Ogushi, and S. Luding, Transition rates for slip-avalanches in soft athermal disks under quasistatic simple shear deformations, Soft Matter **15**, 3487 (2019).
[15] E. E. Ferrero and E. A. Jagla, Elastic interfaces on disordered substrates: From mean-field depinning to yielding, Phys. Rev. Lett. **123**, 218002 (2019).
[16] N. Oyama, H. Mizuno, and A. Ikeda, Unified view of avalanche criticality in sheared glasses, Phys. Rev. E **104**, 015002 (2021).
[17] N. Oyama, H. Mizuno, and A. Ikeda, Instantaneous normal modes reveal structural signatures for the Herschel-Bulkley rheology in sheared glasses, Phys. Rev. Lett. **127**, 108003 (2021).
[18] N. Oyama, H. Mizuno, and A. Ikeda, Shear-induced criticality in glasses shares qualitative similarities with the Gardner phase, Soft Matter **19**, 6074 (2023).
[19] J. P. Sethna, K. A. Dahmen, and C. R. Myers, Crackling noise, Nature (London) **410**, 242 (2001).
[20] J. Lin, E. Lerner, A. Rosso, and M. Wyart, Scaling description of the yielding transition in soft amorphous solids at zero temperature, Proc. Natl. Acad. Sci. U.S.A. **111**, 14382 (2014).
[21] W. H. Herschel and R. Bulkley, Konsistenzmessungen von Gummi-Benzollösungen, Kolloid Z. **39**, 291 (1926).
[22] σ_Y is the value in the thermodynamic limit and can be estimated from the system-size dependence of $\langle\sigma\rangle$ under quasistatic shear [17,20].
[23] See Supplemental Material at http://link.aps.org/supplemental/10.1103/PhysRevLett.132.148201 for details of theoretical backgrounds and critical parameters estimation, which includes Ref. [24].
[24] J. T. Clemmer, K. M. Salerno, and M. O. Robbins, Criticality in sheared, disordered solids. I. Rate effects in stress and diffusion, Phys. Rev. E **103**, 042605 (2021).
[25] S. D. Bembenek and B. B. Laird, Instantaneous normal modes and the glass transition, Phys. Rev. Lett. **74**, 936 (1995).
[26] R. M. Stratt, The instantaneous normal modes of liquids, Acc. Chem. Res. **28**, 201 (1995).
[27] J. D. Gezelter, E. Rabani, and B. J. Berne, Can imaginary instantaneous normal mode frequencies predict barriers to self-diffusion?, J. Chem. Phys. **107**, 4618 (1997).
[28] S. D. Bembenek and B. B. Laird, Instantaneous normal modes analysis of amorphous and supercooled silica, J. Chem. Phys. **114**, 2340 (2001).

[29] I. Kriuchevskyi, T. W. Sirk, and A. Zaccone, Predicting plasticity of amorphous solids from instantaneous normal modes, Phys. Rev. E **105**, 055004 (2022).
[30] D. Bonn, M. M. Denn, L. Berthier, T. Divoux, and S. Manneville, Yield stress materials in soft condensed matter, Rev. Mod. Phys. **89**, 035005 (2017).
[31] A. Nicolas, E. E. Ferrero, K. Martens, and J.-L. Barrat, Deformation and flow of amorphous solids: Insights from elastoplastic models, Rev. Mod. Phys. **90**, 045006 (2018).
[32] M. P. Allen and D. J. Tildesley, *Computer Simulation of Liquids* (Oxford University Press, New York, 1987).
[33] The elastic waves travel less than a distance of 0.005 within a numerical step.
[34] C. E. Maloney and M. O. Robbins, Evolution of displacements and strains in sheared amorphous solids, J. Phys. Condens. Matter **20**, 244128 (2008).
[35] A. Lemaître and C. Maloney, Sum rules for the quasi-static and visco-elastic response of disordered solids at zero temperature, J. Stat. Phys. **123**, 415 (2006).
[36] K. M. Salerno, C. E. Maloney, and M. O. Robbins, Avalanches in strained amorphous solids: Does inertia destroy critical behavior?, Phys. Rev. Lett. **109**, 105703 (2012).
[37] Consistently with the observations, a scaling relation $\hat{D}_0 \sim L^{d-d_f}$ was proposed [12].
[38] G. Picard, A. Ajdari, F. Lequeux, and L. Bocquet, Elastic consequences of a single plastic event: A step towards the microscopic modeling of the flow of yield stress fluids, Eur. Phys. J. E **15**, 371 (2004).
[39] A. Lemaître, C. Mondal, M. Moshe, I. Procaccia, S. Roy, and K. Screiber-Re'em, Anomalous elasticity and plastic screening in amorphous solids, Phys. Rev. E **104**, 024904 (2021).
[40] D. Hexner, A. J. Liu, and S. R. Nagel, Two diverging length scales in the structure of jammed packings, Phys. Rev. Lett. **121**, 115501 (2018).
[41] H. Shao, W. Guo, and A. W. Sandvik, Quantum criticality with two length scales, Science **352**, 213 (2016).